Sustainability in Environment
ISSN 2470-637X (Print) ISSN 2470-6388 (Online)
Vol. 11, No. 3, 2026
www.scholink.org/ojs/index.php/se

Original Paper

Effect of Black Carbon on the Gas-Phase Oxidation of SO_2 by H_2O_2 to Form Sulfate

Wenyao Zhang[1]

[1] Nanjing University of Information Science and Technology, Nanjing, Jiangsu, China

Received: March 27, 2026 Accepted: April 29, 2026 Online Published: May 20, 2026

doi:10.22158/se.v12n3p28 URL: http://dx.doi.org/10.22158/se.v12n3p28

Abstract

A common carbonaceous aerosol in the atmosphere that absorbs light is called black carbon (BC). During haze situations, it can be crucial to the development of sulfate. In this work, we used a flow tube reactor system to replicate the gas-phase oxidation of SO_2 by H_2O_2 in the presence of BC. We looked into the fundamental process as well. According to our findings, BC greatly encourages the development of sulfates. Stronger UV light intensity, higher BC mass concentration, and higher H_2O_2 concentration all promote this amplification. The reaction exhibits pseudo-first-order kinetics, according to kinetic analysis. When BC is present, the absorption coefficient rises to 2.728×10^{-7}, indicating a significant increase in reaction rate. We identified the microscopic process by XPS analysis and radical scavenging studies. The "pre-adsorption–oxidation" route is followed in the production of sulfate. In particular, SO_2 initially adsorbs onto the surface of BC. The reaction energy barrier is subsequently lowered by electron transfer, enabling further oxidation to sulfate. Additionally, BC catalyzes the breakdown of H_2O_2 to produce singlet oxygen ($^1O_2$), superoxide radicals ($\cdot O_2^-$), and hydroxyl radicals ($\cdot OH$). The conversion of SO_2 is accelerated by these extremely reactive oxygen species. This study emphasizes how important BC is in encouraging the development of atmospheric sulfates. It offers a fresh theoretical foundation for improving our comprehension of atmospheric sulfate production processes.

Keywords

Black carbon, SO_2, H_2O_2, gas-phase oxidation, sulfate

1. Introduction

One of the main components of fine particulate matter ($PM_{2.5}$) is atmospheric sulfate. It has a major impact on regional climate, human health, and air quality (Zhang, Wang, Guo et al., 2015). The exponential rise of sulfate during large pollution episodes is frequently not explained by conventional

atmospheric chemistry models (Xie, Gunnar, Huizheng Che, et al., 2025). This implies that unidentified unconventional formation paths may exist. One significant aqueous-phase oxidant in the atmosphere is H_2O_2. S(IV) can be efficiently oxidized to sulfate by the ·OH radicals produced during its breakdown. During periods of haze, this procedure is very important (Zhang, Zheng, Tong et al., 2019).

The primary source of black carbon (BC) is incomplete combustion of biomass and fossil fuels (Guo, Lu, Qiu et al., 2024). The environment is filled with it. BC has a delocalized π-conjugated electron network, a large number of surface defect sites, and functional groups that contain oxygen (Liu, Liu, Zhang et al., 2024). Because of these characteristics, BC may function as a catalyst in heterogeneous processes. According to earlier research, BC can encourage SO_2 to be oxidized by NO_2 or O_3. Its precise function and the underlying microscopic process in the crucial gas-phase SO_2 oxidation route by H_2O_2 are still unknown, though (Ryan, James, Laura-Hélèna et al., 2024).

In light of this information gap, this study used a flow tube reactor to model the gas-phase oxidation of SO_2 by H_2O_2 in the presence of BC. We thoroughly examined how light conditions, H_2O_2 concentration, and BC mass concentration affected sulfate production (Zhou, Yang, Kang, et al., 2024). We investigated the mechanism of BC in this reaction in detail using XPS characterisation, radical scavenging studies, and kinetic analysis. Our objective is to offer a fresh scientific foundation for comprehending the creation of heterogeneous sulfates in the atmosphere (Zhao, Zhao, Zheng, et al., 2024).

2. Experimental Section

2.1 Experimental Materials

The BC utilized in this investigation was made in a lab using biomass, specifically rice straw. Oxygen-limited pyrolysis at 973 K was used to create it. Sinopharm Group supplied the nitrotetrazolium blue chloride (NBT), terephthalic acid (TA), and H_2O_2 (30%). Nanjing Jiangte Gas Co., Ltd. provided high-purity N_2 and SO_2 standard gas (500 ppmv, balanced with N_2).

2.2 Characterization of BC

A GeminiSEM 300 scanning electron microscope was used to examine BC morphology. An automatic gas adsorption analyzer (BET) was used to measure specific surface area. A SmartLab SE X-ray diffractometer (XRD) was used to examine the crystal structure. A Nicolet iS20 Fourier transform infrared spectrometer (FTIR) was used to characterize surface functional groups. A Nexsa X-ray photoelectron spectrometer (XPS) was used to examine the surface elemental chemical states prior to and following the reaction.

2.3 Sulfate Formation Simulation Experiments

A self-designed flow tube reactor setup was used for the experiment. Quartz wool was uniformly loaded with a specific mass of BC. Next, the loaded quartz wool was positioned close to the reaction tube's gas inlet side. The system was purged with N_2 (200 mL/min) for 20 minutes before to the reaction. A nebulizer was then used to introduce 1 mL of H_2O_2 solution at a specified concentration. N_2

(200 mL/min) and SO_2 (20 mL/min) were added to the reactor simultaneously. An SO_2 detector was used to continuously monitor the SO_2 levels at the reactor exit. Over a 15-minute reaction time, data were recorded every 30 seconds. We altered the BC mass (0, 10, 15, 20 mg), the H_2O_2 concentration (9.79×10^{-4}, 4.89×10^{-3}, 9.79×10^{-3}, 1.96×10^{-2} mol/L), and the illumination setting (with or without a 254 nm UV lamp) in order to examine the impacts of various parameters.

2.4 Radical Measurements

DMPO served as the spin trap for the measurement of ·OH and $\cdot O_2^-$. TEMP was employed as the trap for $^1O_2$. BC and H_2O_2 were added to a solution containing the corresponding trap under 254 nm UV light irradiation. At reaction times of 0, 1, 3, 5, and 10 minutes, samples were collected. An EPR spectrometer (Bruker A300) was then used to evaluate the samples. TA was used as a probe for fluorometric measurement of ·OH. A fluorescence spectrophotometer was used for the measurements (emission at 425 nm, excitation at 315 nm). The NBT method was used to quantify O_2^-, and a UV spectrophotometer was used to detect absorbance at 260 nm.

2.5 Kinetic Analysis

The overall flow rate in the flow tube reactor was regulated at 1000 mL/min (N_2: 900 mL/min, SO_2: 100 mL/min). The BC dispersion and H_2O_2 solution were nebulized into the reactor at the same time. Real-time monitoring of the output SO_2 concentration was conducted. Assuming pseudo-first-order reaction kinetics for SO_2 consumption:

$$\mathrm{Ln}\left(\frac{C_0}{C_t}\right)=kt \tag{1}$$

To measure the promoting impact of BC, the uptake coefficient γ was determined as

$$\gamma=\frac{K_0}{K_{BC}} \tag{2}$$

where k_0 is the reaction constant in the absence of BC.

3. Results and Discussion

3.1 Effect of BC on Sulfate Formation

3.1.1 Effect of BC Mass Concentration

The variation in outflow SO_2 concentration over time under various BC masses is depicted in Figure 1a. At 10 minutes, the outlet SO_2 concentration dropped from 41.7 ppm to 21.7 ppm as the BC mass rose from 0 mg to 20 mg. This suggests that sulfate production has significantly increased. The catalytic efficiency (EF) rose from 0.144 to 0.480, as seen in Figure 1b. More surface active sites and oxygen-containing functional groups are provided by a greater BC mass, which causes this increase. These characteristics increase SO_2's capacity for electron transport and adsorption, hastening its oxidation.

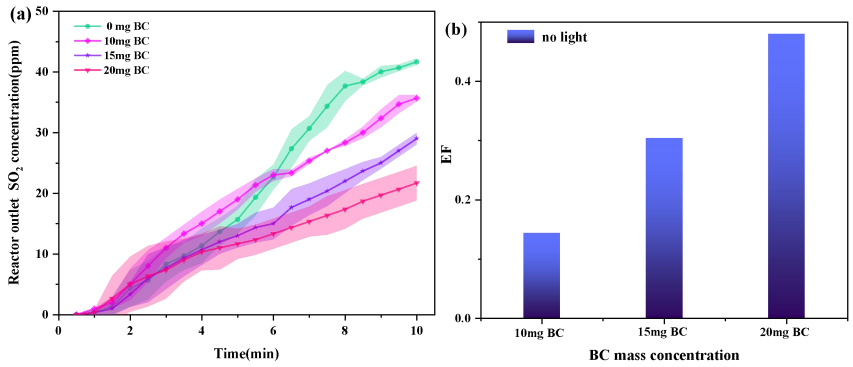

Figure 1(a). Effect of Different BC Mass Concentrations on Sulfur Dioxide Oxidation and (b) Catalytic Efficiency EF

3.1.2 Effect of H_2O_2 Concentration

Figure 2 illustrates how the exit SO_2 concentration dropped from 36.0 ppm to 23.7 ppm after 10 minutes of reaction as the H_2O_2 concentration rose from 9.79 × 10^{-4} mol/L to 1.96 × 10^{-2} mol/L. In the meantime, the EF value rose from 0.136 to 0.432. The system produced more ·OH as the concentration of H_2O_2 increased. Consequently, the conversion of SO_2 to sulfate was accelerated by strengthening the aqueous-phase oxidation capacity.

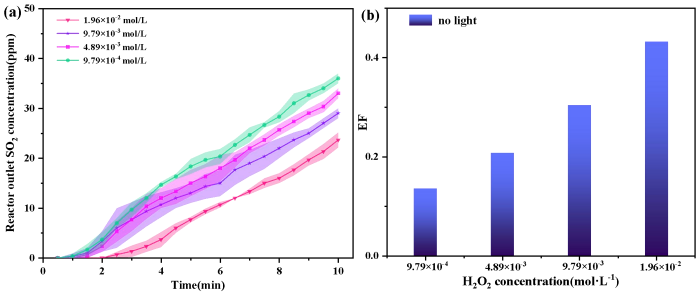

Figure 2(a). Effect of BC on Sulfate Formation at Different H_2O_2 Concentrations and (b) Catalytic Efficiency EF

3.1.3 Effect of Light

The EF values for BC masses of 10, 15, and 20 mg under UV light irradiation are 0.232, 0.400, and 0.592, respectively, as shown in Figure 3. All of these values are greater than those obtained in the dark (0.144, 0.304, and 0.480). More ·OH is produced when illumination encourages the photolysis of H_2O_2. Furthermore, it stimulates photogenerated electron-hole pairs on the BC surface, which encourages the production of ROS. The performance of catalytic oxidation is improved by both effects.

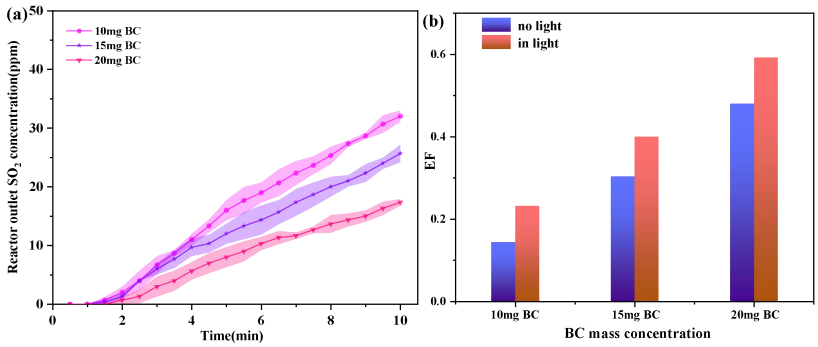

Figure 3(a). Effect of Different BC Mass Concentrations on Sulfate Formation under Light Conditions and (b) Catalytic Efficiency EF

3.2 Reaction Kinetic Analysis

A pseudo-first-order reaction kinetics model is fitted to the data from Figure 1 in Figure 4. Good linear relationships are seen in the fitted curves for various BC masses ($R^2 > 0.99$). As BC mass increases, the reaction rate constant k drops ($k_0 = 3.7 \times 10^{-1}$, $k_1 = 1.8 \times 10^{-1}$, $k_2 = 1.1 \times 10^{-1}$, $k_3 = 7.3 \times 10^{-2}$ s^{-1}). This suggests that the rate of SO_2 consumption is rising. 2.065 (10 mg), 3.332 (15 mg), and 5.082 (20 mg) are the computed uptake coefficients γ. The EF values at the end of the reaction (0.144-0.480) are significantly lower than these values. This result implies that BC's actual kinetic increase of the reaction rate is more important. This effect can be underestimated by the endpoint concentration technique.

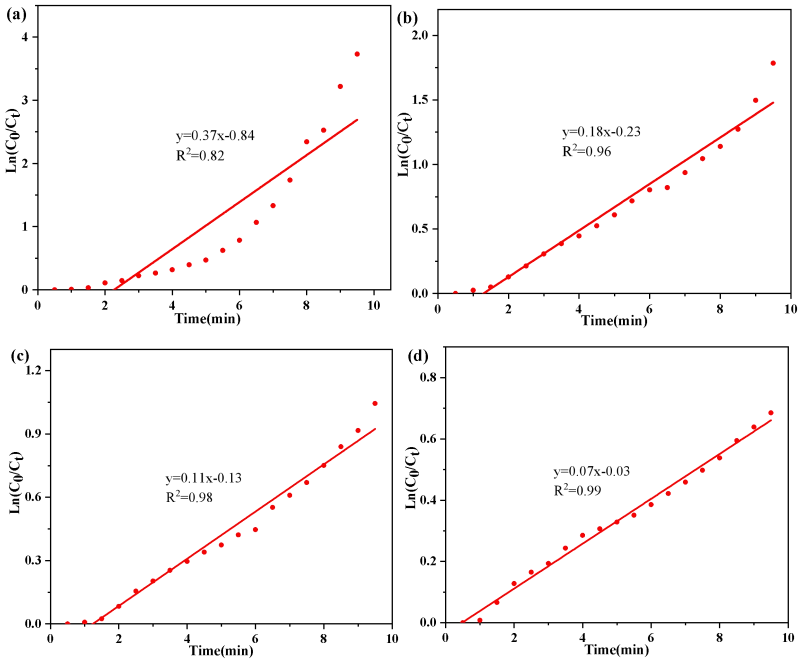

Figure 4. Linear Fitting of First-order Kinetics under Conditions of 0-20 mg BC

3.3 Characterization of BC

BC particles are porous spheres or irregularly shaped blocks, as seen in the SEM picture (Figure 5). They have a lot of pore structures and rough surfaces. According to BET (Figure 6) study, BC has a specific surface area of 270.7 m^2/g. The majority of the pore structure is mesoporous. Amorphous carbon is characterized by a large diffuse peak at $2\theta \approx 24°$ in the XRD pattern (Figure 7). Functional groups such as -OH (3400 cm^{-1}), C=C (1600 cm^{-1}), and C=O (1000-1080 cm^{-1}) are present on the BC surface, according to the FTIR spectrum (Figure 8). Numerous active sites on BC are made possible by these structural and chemical characteristics, which aid in the adsorption and catalytic conversion of SO_2.

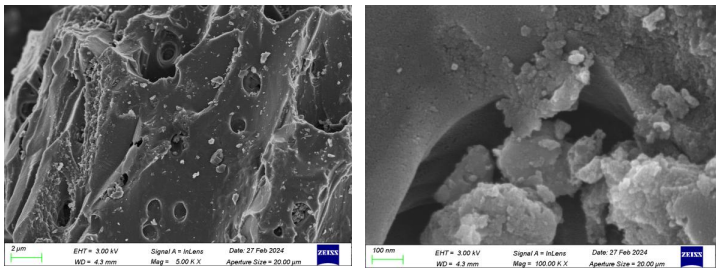

Figure 5. SEM Image of BC

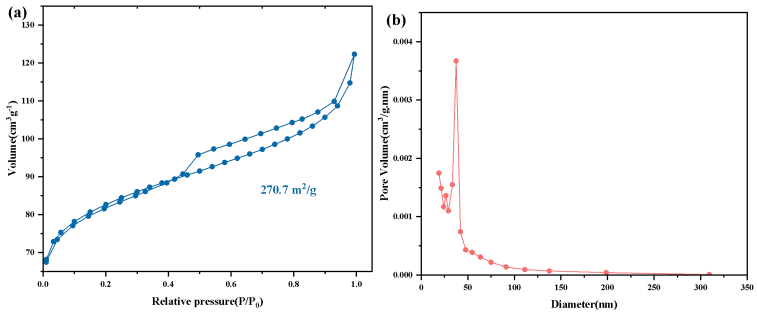

Figure 6. N_2 Adsorption-desorption Isotherms and Pore Size Distribution of BC

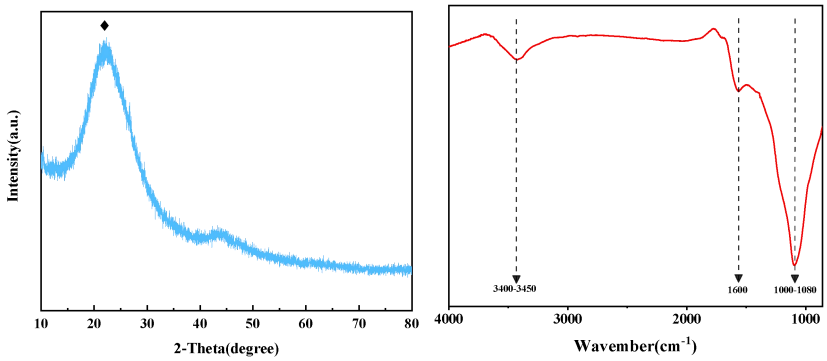

Figure 7. XRD Pattern of BC and Figure 8 FTIR Spectrum of BC

3.4 Identification and Quantification of Radicals

The distinctive peaks of the DMPO-·OH adduct (1:2:2:1 quartet), the DMPO-·O_2^- adduct (sextet), and the TEMP-$^1O_2$ adduct (triplet) are considerably stronger in the presence of BC than in the BC-free

control group, according to the EPR spectral results (Figures 9). According to quantitative analysis, the amounts of ·OH and $\cdot O_2^-$ produced in the BC-containing system after 10 minutes of reaction are 0.179 mmol/L and 0.034 mmol/L, respectively. Compared to the blank group, these values are significantly higher. This suggests that BC efficiently catalyzes the breakdown of H_2O_2, producing several extremely reactive ROS. The primary species responsible for the quick oxidation of SO_2 to sulfate are these ROS.

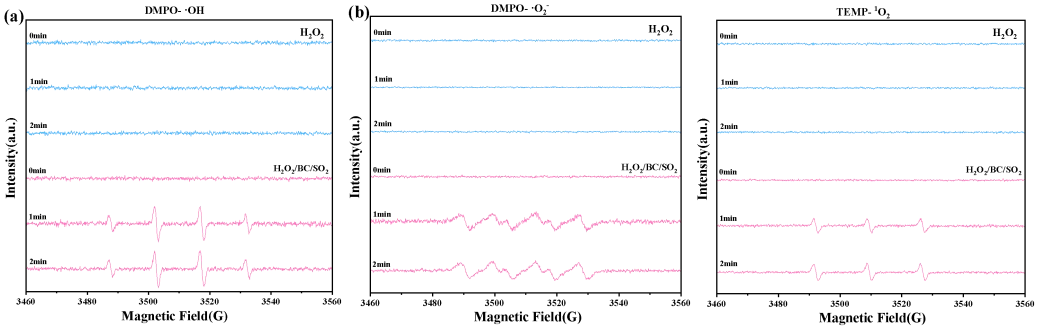

Figure 9. EPR Spectra of H_2O_2 and BC under Different Reaction Conditions: (a) DMPO-·OH (b) DMPO-$\cdot O_2^-$ and (c) TEMP-$^1O_2$

3.5 XPS Analysis of BC Before and After Reaction

The tiny SO_2 oxidation process on the BC surface was discovered via XPS analysis. The clean BC surface showed no sulfur signal in the S 2p spectrum (Figure 10a). A peak emerged at about 166-168 eV following the reaction with SO_2. Adsorbed HSO_3^-/SO_3^{2-} (S(IV)) is responsible for this peak. A new peak at ~169.7 eV, which corresponds to SO_4^{2-} (S(VI)), emerged when H_2O_2 was introduced to the solution. This suggests that SO_2 first adsorbs onto the BC surface to create sulfite, which is subsequently oxidized to sulfate, indicating a "pre-adsorption–oxidation" process on the BC surface.

The C 1s peak of pristine BC is located at 284.6 eV (C=C) in the C 1s spectrum (Figure 10b). The C 1s peak moves to a higher binding energy following SO_2 adsorption. This shows that electrons are transferred from BC to the adsorbed SO_2. The C 1s peak changes back to a lower binding energy when sulfate is produced, indicating that electron back-donation takes place. The chemical environment of oxygen-containing functional groups (C=O, C-OH) on the BC surface changes following the reaction, as further shown by the O 1s spectrum (Figure 10c). These groups take part in the oxidation process directly. All of these findings demonstrate that BC lowers the energy barrier for the conversion of S(IV) to S(VI) by acting as an electron transfer mediator in the process.

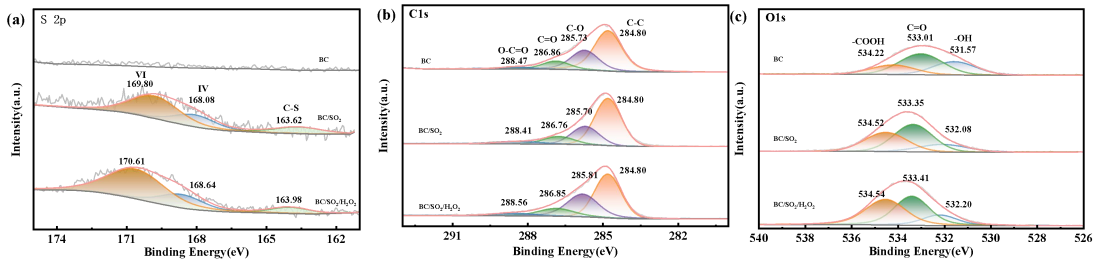

Figure 10. XPS Spectra of BC before and after the Reaction: (a) S 2p, (b) C 1s, (c) O 1s

4. Conclusion

This investigation demonstrates the important catalytic function of BC in the oxidation of SO_2 by H_2O_2 to produce sulfate. According to the results of our experiments, BC successfully encourages the creation of sulfate. Stronger UV light intensity, higher BC mass concentration, and higher H_2O_2 concentration all promote this amplification. According to kinetic analysis, the reaction has pseudo-first-order reaction kinetics. The absorption coefficient rises to 2.728×10^{-7} when BC is present, indicating a significant increase in the response rate in a heterogeneous environment. Sulfate production on the BC surface follows a "pre-adsorption – oxidation" route, according to mechanistic investigations.In particular, SO_2 initially adsorbs onto BC surface active sites. The reaction energy barrier is subsequently lowered by electron transfer, enabling further oxidation to sulfate. Meanwhile, BC catalyzes the breakdown of H_2O_2 to form extremely reactive oxygen species, including hydroxyl radicals (·OH), superoxide radicals ($\cdot O_2^-$), and singlet oxygen ($^1O_2$). The conversion of SO_2 to sulfate is accelerated by these radicals. This work emphasizes BC's critical catalytic function in the atmospheric heterogeneous sulfate production process. It offers a fresh theoretical framework for comprehending the quick sulfate production process during haze occurrences.

References

Guo, Z. Y., Lu, K. D., Qiu, P. X. et al. (2024). Quantifying SO_2 oxidation pathways to atmospheric sulfate using stable sulfur and oxygen isotopes: laboratory simulation and field observation. *Atoms. Chem. Phys.*, *24*(4), 2195-2205.

Liu, L. Y., Liu, X., Zhang, R. F. et al. (2024). Global Impact of Particulate Nitrate Photolysis on Fine Sulfate Aerosol. *Environ. Sci. Technol.*, *11*(9), 961-967.

Ryan, F., James, E. L., Laura-Hélèna, R. et al. (2024). Chemical properties and single-particle mixing state of soot aerosol in Houston during the TRACER campaign. *Atmos. Chem. Phys.*, *24*(7), 3953-3971.

Xie, X. N., Gunnar, M., Che, H. Z. et al. (2025). Anthropogenic sulfate-climate interactions suppress dust activity over East Asia. *Commun. Earth Environ.*, *6*(1), 2706-2712.

Zhang, Q., Zheng, Y. X., Tong, D. et al. (2019). Drivers of improved $PM_{2.5}$ air quality in China from 2013 to 2017. *Proc. Natl. Acad. Sci. U.S.A.*, *116*(49), 24463-24469.

Zhang, R., Wang, G., Guo, S. et al. (2015). Formation of urban fine particulate matter. *Chem. Rev.*, *115*(10), 3803-3855.

Zhao, W. X., Zhao, Y., Zheng, Y. et al. (2024). Long-term variability in black carbon emissions constrained by gap-filled absorption aerosol optical depth and associated premature mortality in China. *Atmos. Chem. Phys.*, *24*(11), 6593-6612.

Zhou, Y. W., Yang, J. H., Kang, S. X. et al. (2024). Black carbon aerosols impact snowfall over the Tibetan Plateau. *Geosci. Front.*, *16*(2), 101978.